Journal of Water Process Engineering 56 (2023) 104559

Contents lists available at ScienceDirect

Journal of Water Process Engineering

journal homepage: www.elsevier.com/locate/jwpe

Retention of microplastics by interspersed lagoons in both natural and constructed wetlands

Mirco Mancini [a,*], Luca Solari [a], Jordi Colomer [b], Teresa Serra [b]

[a] Department of Civil and Environmental Engineering, University of Florence, Via S. Marta 3, 50139 Florence, Italy
[b] Department of Physics, University of Girona, Campus Montilivi, 17003 Girona, Spain

A R T I C L E I N F O

Keywords:
Emerging contaminants
Unidirectional flow
Nature-based solutions
Shallow aquatic vegetation
Treated water

A B S T R A C T

Natural wetlands, the transitional zones found between the land and the sea, are considered hot spots for plastic accumulation. Constructed wetlands (CW) attempt to mimic these natural wetlands in order to provide potential Nature-Based Solutions (NBS) for reducing microplastic (MP) contamination in wastewater treatment plants, and mitigating MP pollution in rivers. In this work, the role played by an interspersed lagoon surrounded by aquatic vegetation (*Juncus Maritimus*) in retaining MP was investigated using experimental laboratory simulations. Four MP types (125–500 μm and 500–1000 μm PA fragments, 2 mm PET fibers and 5 mm PET fibers) along with suspended sediments were injected into the model wetland to study their transport throughout the system. Five different vegetated patch lengths surrounding the lagoon were considered (L_P). Results showed that aquatic vegetation protected wetlands from PA fragments and PET fibers by increasing the dispersion of the particle-laden flow and consequently MP sedimentation. When the use of vegetated patches was coupled with an interspersed lagoon, MP retention rates were maximized (with total percentages of 88 ± 3 % and 99 ± 1.5 % for PA fragments and PET fibers, respectively), suggesting that CW are a potential NBS for trapping MP pollution from specific sources.

1. Introduction

Plastic and chiefly microplastic (MP) pollution is now a problem common to all environmental compartments [1]. Both marine and freshwater environments are of great interest to the scientific community in that they present ever-growing concentrations of plastic particles [2–4]. Plastic pollution in inland waters is directly correlated to the population and economic levels of the area in question [5,6]. Rivers represent preferential ways by which discarded plastic fragments from land sources reach oceans and seas [7–9]. That said, most of the plastic entering a river system is trapped by vegetation and buried under the riverbed sediment, thus increasing its residence time in inland water systems, and often never reaching the open sea [10]. According to Gallitelli et al. [11], the ability of aquatic plants to capture MP manly depends on plant density rather than the size of the plastic particles. Nonetheless, plastic particles suspended in the water column are subject to mechanical, chemical, and biological degradation processes [12–14], reaching sizes of tens of microns or less and, depending on their concentration levels, increasing the negative impact they have on aquatic life [15]. Furthermore, exposure to UV-light and weathering can accelerate the degradation process [16,17]. MP degradation causes an increase of MP in the exposed area, potentially increasing chemical reactivity. Thus, MPs are also responsible for transporting biological and chemical contaminants by adsorption [18] and therefore also become vectors for particle-bound chemicals, especially those chemicals that were used to produce plastic material in the first place [19].

MP can also interact with suspended sediments (SS). For example, slow-settling MP particles scavenging by fast-settling sediment particles have been found to increase the vertical transport of MP to the bottom of the water column [20]. Likewise, in a unidirectional flow regime, the increase in SS concentration increases MP sedimentation rates thanks to MP scavenging by SS, which then leads to a segregation of MP particles along the patch of the MP plume [21]. Mancini et al. [21] also found that the impact SS has on the sedimentation rate of MP depended on the type, size, and shape of the MP particles. In sum, the transport of MP in water environments is not only influenced by MP density, shape, and size (which determine MP settling velocity), but also by the hydrodynamics of the aquatic systems [20,22] which, in turn, may affect MP settling velocity [23–25]. MPs are expected to have a high settling rate under low flow velocities and calm conditions [20] in comparison to turbulent aquatic systems.

* Corresponding author.
E-mail address: mirco.mancini@unifi.it (M. Mancini).

https://doi.org/10.1016/j.jwpe.2023.104559
Received 9 August 2023; Received in revised form 9 November 2023; Accepted 11 November 2023
Available online 20 November 2023

Nomenclature

A	Frontal area of the vegetation per unit volume
a	Longest axes of measured particles
ADV	Acoustic Doppler Velocimeter
b	Intermediate axes of measured particles
c	Shortest axes of measured particles
C	Particle concentration
C_{CUM}	Cumulative size curve of particles
C_i	Particle concentration at each measuring section i
C_{i-1}	Particle concentration at the measuring section i-1
C_L	Particle concentration in the lagoon
C_{L_MAX}	Maximum particle concentration in the lagoon
C_{MAX}	Maximum particle concentration
C_{MP}	Microplastic concentration
C_{MP_MAX}	Maximum microplastic concentration
C_{sed}	Sediment concentration
CSF	Corey Shape Factor
CW	Constructed wetland
C_1	Dimensionless coefficient
C_2	Dimensionless coefficient
D	Diameter of the source of the plume at the inlet
d	Stem diameter
d_{50}	Particle diameter representing the 50 % cumulative percentile value
D*	Dimensionless reference diameter
d_{eq}	Equivalent diameter
D_g	"Modified" representative diameter
g	Gravity acceleration
E	Shape factor
H	Stems height
h_w	Water height in the shallow water areas
K	Microplastics sedimentation rate
k	von Karman constant
L	Flume width
Lisst	Laser In-Situ Scattering and Transmissometry
l_m	Characteristic length scale of the plume injection
L_P	Vegetated patch length
M_0	Momentum flux
MBR	Membrane bioreactors
MP	Microplastic
n	Canopy density
n_{GM}	Gauckler–Manning coefficient
n_s	Dimensionless coefficient
NBS	Nature-Based Solutions
P	Rouse number
PA	Polyamide
PE	Polyethylene
PET	Polyethylene terephthalate
PP	Polypropylene
PS	Polystyrene
Q_0	Total buoyancy flux
R	Characteristic diameter of the flume
R_s	Submerged relative density
Re	Reynolds number
SPF	Solid plant fraction
SS	Suspended Sediments
U_c	Mean current flow velocity
u*	Shear velocity
V_{front}	Mean front velocity of the plume
W	Dimensional settling velocity
W*	Dimensionless settling velocity
W_0	Plume injection velocity at the source
α	Dimension correction factor
Δ	Characteristic distance reached by each MP
Δ_{b0}	Buoyancy of the plume discharged
Δ_{MAX}	Maximum characteristic distance reached by each MP
μ	Water viscosity
ρ	Water density
ρ'	Density of the particle laden plume
ρ_p	Particle density
ν	Fluid kinematic viscosity

Shallow water bodies (i.e., wetlands, coastal lagoons, and estuaries) promote the biodiversity of different species of flora and fauna [26] and facilitate the reproduction and growth of microorganisms, aquatic plants, and animals [27]. Lagoons interspersed in wetlands provide valuable recognized ecosystem services by improving human living conditions, increasing agricultural production, reducing the effects of flooding events, and regulating the climate [28]. Wetlands represent the link between rivers and marine environments and so not only do most of the plastic and MP particles from inland waters migrate through them before entering the sea, so too do the particles coming from marine environments [29].

In recent years, several studies have been carried out to quantify and characterize MP in shallow water systems around the word [29–33]. High concentration of MP have been found buried in sediment beds [28,34,35], trapped in seagrasses and macroalgae [36,37], remaining in suspension in the water column, or ingested by aquatic organisms from zooplankton [38] to large organisms like fish [39,40] and mollusks [41,42]. According to the recent review by Garcés-Ordóñez et al. [28], the most common shapes of MP found in coastal lagoon environments are fibers and fragments which are mainly transparent blue colors. Garcés-Ordóñez et al. [28] reported that polyethylene (PE), polypropylene (PP) and polyester (PS), were the most abundant polymer compositions, followed by polyethylene terephthalate (PET) and polyamide (PA).

In addition to shallow water bodies, constructed wetlands are now considered as nature-based solutions for the mitigation and disinfection of pollution, and to prevent microplastic pollution [43] in river systems. Vegetation cover and stem density play an important role in retaining MPs in constructed wetlands, presumably modifying hydrodynamics [44,45]. Constructed wetlands appear to efficiently remove up to 50 % of MP depending on MP type [46]. However, even higher MP removal efficiencies have been observed in surface constructed wetlands – 88 % [47] and horizontal subsurface flow constructed wetlands – 100 % [48], indicating their suitability for being used as tertiary treatments for MP pollution.

Despite all the work carried out in both shallow water bodies and constructed wetlands (CW), a gap in the knowledge about the role lagoons play in retaining MP remains. Because lagoons are surrounded by aquatic vegetation, this makes the performance of the lagoon-vegetation system even more complex and consequently not only the role vegetation in a lagoon plays in retaining microplastic particle needs to be better addressed, but so too whether the lagoon itself is sheltered or unsheltered by vegetation.

Through a series of laboratory experiments, the present work aims to investigate the role wetland lagoons (sheltered or unsheltered by vegetation) play in retaining MP and determine the conditions in which vegetation is able to protect interspersed lagoons from MP pollution. For this purpose, a lagoon was built in a unidirectional flow flume and the emergent aquatic vegetation (*Juncus maritimus*) placed around the lagoon aimed to mimic real wetland conditions. Different patch lengths of the vegetation surrounding the lagoon are explored to determine the sheltering effect they have on the lagoon. Four different types of MP (PA fragments and PET fibers, in two size ranges) are considered for experiments, thus covering a wide range of plastic densities and shapes. Finally, the relevance of the study findings in providing guidance to optimize the ecosystem services provided by wetlands is discussed. Likewise, a discussion on developing more efficient strategies for maintaining and preserving natural wetlands from plastic pollution is also included in the discussion section of the manuscript.

2. Materials and method

2.1. Flume set-up

Experiments were carried out in a 500 cm × 40 cm × 50 cm laboratory flume. At the entrance of the flume a honeycomb was used to straighten the flow produced at the inlet [49], while at the outlet an 18 cm high gate ensured a constant flow level (Fig. 1). The flume had a storage tank that allowed the water to recirculate using a pump with a valve to control the flow in the flume. Two 10-cm high platforms 120 cm long at the base and 100 cm long at the top were constructed and placed in the flume, creating a deep zone between them to represent a V-shaped lagoon (Fig. 1). The platforms represented shallow water areas with or without vegetation depending on the experiment. The space between the platforms created a lagoon that was 18 cm long at the base and 38 cm long at the top and 11 cm deep from the upper part of the shallow zones to the base of the flume. Two 100 cm × 40 cm × 1 cm bases were placed on top of each shallow zone. The bases were perforated with 0.6 cm diameter holes, where plant stems were then distributed.

In the shallow zones, a water height $h_w = 10$ cm was considered. The vegetation in the shallow areas consisted of stems of real *Juncus maritimus* vegetation (Fig. 1), typical of river floodplain zones and saltmarshes, which had been collected near the Ter River (Catalonia, North-East Spain). Three to four *Juncus maritimus* stems were attached and tied with tape to build a 0.6 cm thick plant that fitted into the perforated holes in the bases. A canopy density of $n = 1344$ shoots m^{-2} was considered, i.e., in line with the canopy densities found in saltmarshes [50,51]. From the canopy density (n) and the value of the stem diameter (d) the percentage of the area covered by the vegetation in the shallow vegetated areas, i.e., the solid plant fraction $SPF = n\pi d^2/4 = 3.8$ %, [52,53] was obtained. Stems were cut to 20 cm long to ensure that the vegetation was emergent and were randomly distributed using a

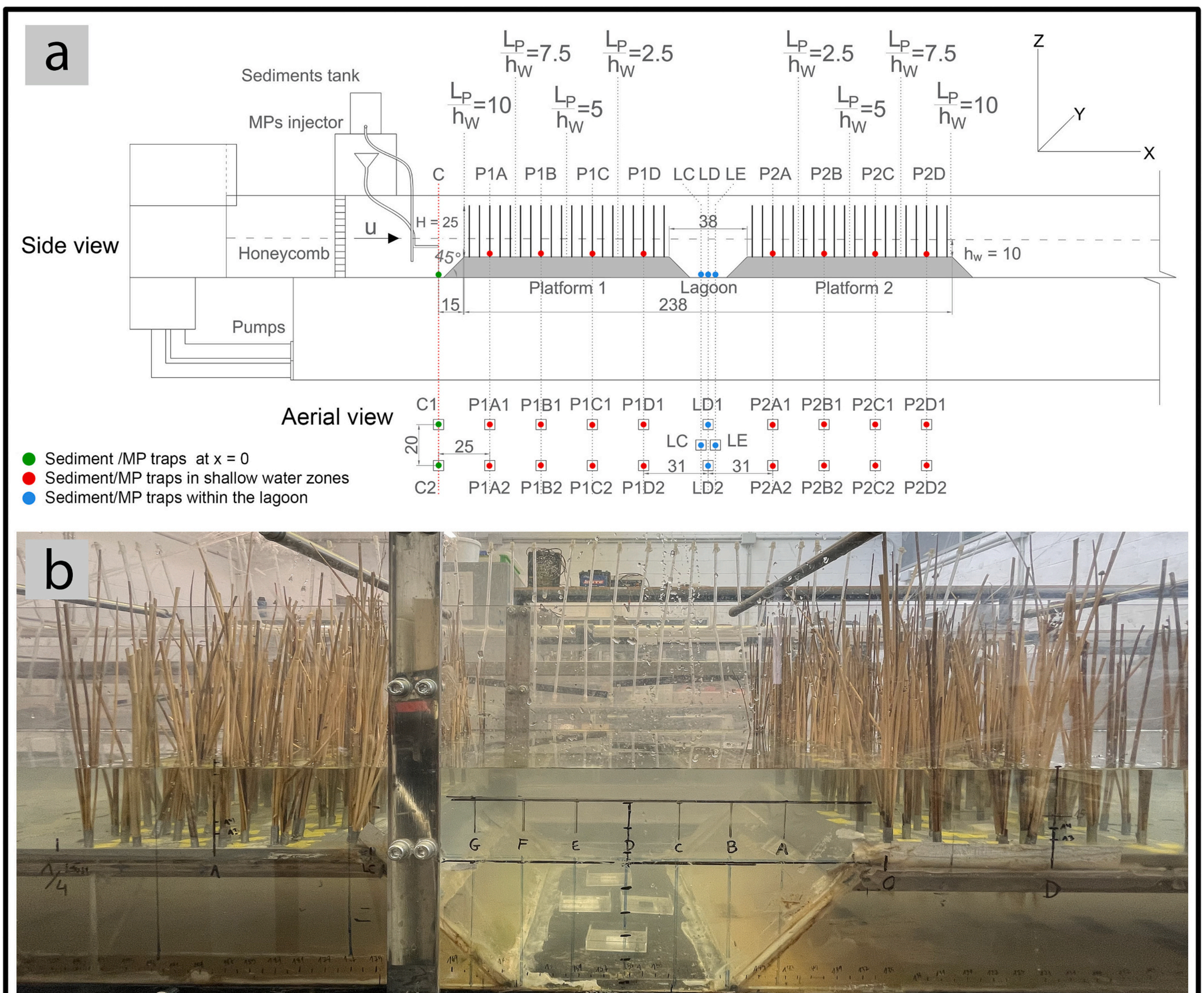

Fig. 1. Scheme of the experimental flume: Side and aerial views of flume with trap sampling positions in shallow water areas (P1A to P2D) and at the bottom of the lagoon (LC, LD, LE). All measurements are in cm. The length of the vegetated canopy surrounding the lagoon was given as times the water depth in the shallow water areas (h_w). A photograph of the lagoon and the surrounding vegetation in the flume is included below the scheme.

computer function [52,54,55]. Therefore, the flume set-up was divided into three zones: a lagoon with two adjacent shallow vegetated areas.

Twelve sampling sections along the main axis of the flume (at x = 0 cm, 25 cm, 50 cm, 75 cm, 100 cm, 128.5 cm, 131 cm, 133.5 cm, 162 cm, 187 cm, 212 cm, and 237 cm) were considered. x = 0 cm was set at section C, i.e., at the injection point. The flow in the flume was kept constant for all the experiments carried out in this study. The flow velocity was measured at the same x positions as where the sediment traps were situated using a laboratory Acoustic Doppler Velocimeter (ADV, 16 MHz, SonTek Inc.) that measured the three components of flow velocity at each sampling point. The ADV was placed in the flume at a selected depth (z) and position along the main axis of the flume (x) in a downward-looking configuration. All measurements were taken at the center of the flume in the transversal direction (y = 0 cm, Fig. 1) and at 3 cm above the bottom in the shallow water testing area. Data was collected with a PC linked to the ADV. Measurement frequency was 50 Hz and each measurement lasted 5 min, resulting in a set of 15,000 data points. The ADV measured at a single point in every measurement in a sampling volume of 0.09 cm^3 situated 5 cm from the ADV probe tip. The temporal mean velocity of the x-component at each position was calculated as the mean value of the 15,000 measurements. In the shallow zone, the mean current velocity of the flow was $U_c = 1.2 \pm 0.2$ cm/s. The Reynolds number of the flow in the flume ($Re = \rho U_c R/\mu = 2277$) was calculated assuming the characteristic diameter of the flume (R) as $R = (HL)^{0.5}$, where L is the width of the flume, ρ is the water density, and μ is the water viscosity, resulting in a transitional flow regime very close to the laminar regime.

2.2. Experimental procedure

The sediment used was Arizona coarse test dust (ISO 12103-1, Powder Technology Inc., Burnsville, USA; for a complete characterization see "Sediment and MP characteristics" section in the supplementary material). Two sediment traps were situated at each of the nine different distances (at x = 0 cm, 25 cm, 50 cm, 75 cm, 100 cm, 162 cm, 187 cm, 212 cm, 237 cm) along the main axis of the two shallow water areas (at y = 10 cm and y = −10 cm, considering y = 0 cm at the center of the flume), accounting for a total of eighteen sediment traps in the shallow areas (Fig. 1). A further four sediment traps were placed within the lagoon, as shown in Fig. 1. Sediment traps consisted of 5 cm × 5 cm square glass boxes 0.9 cm height which has been previously positioned at the bottom of the flume (Fig. 1). MP and sediment particles were injected separately to avoid any interaction between them before entering the flume. For this purpose, two mixing tanks were used (C1, C2, Fig. 1). Sediments and MPs were previously diluted in 2 l and 1 l of water, respectively. MPs and sediments were injected into the water, with a total injection time that lasted approximately 2.5 min (total discharge 0.02 l/s). The particle-laden flow injected into the system had a jet-like behavior for a distance $x = l_m < 5.1$ cm and a plume-like behavior for $x = l_m > 5.1$ cm (see Eq. 9 in the "Additional theory" section in the supplementary material). That is, it behaved like a buoyant plume before entering the region under study for all the setups considered. The particle-laden flow dispersed laterally, with a greater dispersion in those cases with vegetation. The front of particles moved along the flume at a velocity of V_{front}. The injection time was considered as the time lapse needed by the particle front to reach the end of the shallow zone in all the cases considered. The time steps when the front of sediment and MP passed each sampling point were acquired. A gate at the inlet of the flume was lowered when the plume of particles reached the end of the second (and last) shallow zone. Then the water was left to remain in the section under study for 600 s so that particles could settle in the system. After this period, all sediment traps were covered with a lid and collected for analysis. The identical procedure was repeated for all experiments to reduce any potential variability. One of the experiments (run number 5, see Table 1) was repeated three times to check for replicability.

A constant sediment concentration (C_{sed}) of 30 g/l was considered at the injection point for all the experiments conducted. Experiments were performed separately for each type of MP (PA fragments and PET fibers, see Table 1) and five different patch lengths ($L_P = 0h_w$, $2.5h_w$, $5h_w$, $7.5h_w$, $10h_w$) of the vegetation in the shallow zone were considered in the experiments; accounting for a total of 16 experiments (Table 1 and Fig. 1).

Table 1
Experimental conditions considered for each experiment (run) carried out are presented in each column of the table: non-dimensional vegetation patch length (L_{patch}/h_w), velocity of the front of the flume (V_{front}, in m/s), MP type, MP particle shape (fragment or fiber), MP density, particle Corey Shape Factor (CSF) and settling velocity of MP particle (W) calculated from equation ((3), see "Additional theory" section in the supplementary material). The superscript 'w' corresponds to experiments carried out without lagoon, while superscript '***' correspond to experiments repeated three times.

Run #	*L_P/h_w [−]*	*V_{front} [m/s]*	*MPs type [−]*	*Shape [−]*	*Density [g/cm³]*	*CSF [−]*	*W [m/s]*	*Dg [μm]*
1	0	0.024	PA	(125-500 μm)	1.14 ± 0.03	0.21–0.42	0.0035 ± 0.001	237 ± 25
2	2.5	0.022	PA	(125-500 μm)	1.14 ± 0.03	0.21–0.42	0.0035 ± 0.001	237 ± 25
3	5	0.020	PA	(125-500 μm)	1.14 ± 0.03	0.21–0.42	0.0035 ± 0.001	237 ± 25
4	7.5	0.018	PA	(125-500 μm)	1.14 ± 0.03	0.21–0.42	0.0035 ± 0.001	237 ± 25
5***	10	0.017	PA	(125-500 μm)	1.14 ± 0.03	0.21–0.42	0.0035 ± 0.001	237 ± 2
6	0	0.024	PET	Fiber (2 mm)	1.38 ± 0.02	0.165	0.006	165 ± 10
7	2.5	0.022	PET	Fiber (2 mm)	1.38 ± 0.02	0.165	0.006	165 ± 10
8	5	0.020	PET	Fiber (2 mm)	1.38 ± 0.02	0.165	0.006	165 ± 10
9	7.5	0.018	PET	Fiber (2 mm)	1.38 ± 0.02	0.165	0.006	165 ± 10
10	10	0.017	PET	Fiber (2 mm)	1.38 ± 0.02	0.165	0.006	165 ± 10
11	0	0.024	PA	(500-1000 μm)	1.14 ± 0.03	0.18	0.02	825 ± 176
12	10	0.017	PA	(500-1000 μm)	1.14 ± 0.03	0.18	0.02	825 ± 176
13	0	0.024	PET	Fiber (5 mm)	1.38 ± 0.02	0.09	0.012	226 ± 4
14	10	0.017	PET	Fiber (5 mm)	1.38 ± 0.02	0.09	0.012	226 ± 4
15^w	0	0.025	PA	(125-500 μm)	1.14 ± 0.03	0.21–0.42	0.0035 ± 0.001	236 ± 25
16^w	0	0.025	PET	Fiber (2 mm)	1.38 ± 0.02	0.165	0.006	165 ± 10

2.3. Measurement procedure

Samples from the sedimentation traps collected at the end of each experiment carried out with small PA fragments (in the range 125 μm to 500 μm) were transferred into glass beakers, brought to a known volume of 100 ml, and immediately analyzed. Sediments (5.27–122 μm) and PA-fragments (144–460 μm) were analyzed with the particle size analyzer Lisst-100× (Laser In-Situ Scattering and Transmissometry, Sequoia Scientific, Inc., Bellevue, WA, see supplementary material for a complete description of its operation) to obtain both the particle size-distribution (Fig. S1) and the cumulative particle size-distribution (Fig. S1). From the sediment particle size distribution and according to the Wentworth [56] grain size classification, sediments were split into three particle ranges: fine/medium silts (5.27 μm–19.8 μm), coarse silts (23.4 μm–63.1 μm) and fine sands (74.5 μm–122 μm). From the PA particle size distribution, small PA fragments were also split in three particle ranges: 125 μm–170 μm, 201 μm- 280 μm and 331–460 μm.

However, since both PET-fibers and PA-fragments (500–1000 μm) were outside the measurable range of the Lisst-100x, they were counted instead. To count them, water samples were transferred into beakers (one for each trap box) and subsequently dried in an oven at 60 °C. Images of PET-fibers and PA-fragments (500–1000 μm) in each baker were acquired and analyzed with the ImageJ software and counted.

2.4. Quality control and assessment

The flume was completely cleaned at the end of each experiment. In each run, water samples were collected in the flume before sediment and MP injection and analyzed with the Lisst-100× to ensure the complete removal of MP particles and sediments from the previous experiment.

2.5. Theory

Particles settle as they are transported along the flume and the volumetric concentration is expected to decrease following an exponential trend, where C can be written as follows:

$$C = C_{MAX} \bullet e^{-Kx} \quad (1)$$

where C is the particle concentration at a distance x from the source, C_{max} is the maximum concentration (near the source), and K is the sedimentation rate (in m^{-1}). From this equation, the characteristic distance reached by each MP (Δ) can be calculated as the distance where C has decreased e times the maximum concentration C_{MAX}.

The horizontal distance up to where particle concentration will decrease (Δ) in a factor e is expected to depend on the length of the vegetation patch (L_P), the settling velocity of particles (W) and the velocity of the particle laden flow front (V_{front}). Two different non-dimensional parameters can be defined (Δ/L_P) and (W/V_{front}). In addition, the shape of the particles can also play an important role in transportation, i.e., elongated particles can align with the streamlines of the flow. To consider the effect the shape of the particle has in its transport along the flume, the Corey Shape Factor (CSF) will be also considered as:

$$\frac{\Delta}{L_P} = f\left(\frac{W}{V_{front}}, CSF\right) \quad (2)$$

3. Results

3.1. Characterization of MP and sediment

PA fragments were very irregular in shape, with those in the size range of 500–1000 μm exhibiting a longer shape (and thus low mean CSF = 0.18 ± 0.04) than smaller PA in the 125–500 μm range (with greater mean CSF = 0.37 ± 0.02). In contrast, PET fibers were comparable to cylinders with their smooth surface and constant diameter of 45 μm, having low CSF = 0.14 ± 0.01 and CSF = 0.08 ± 0.002 for 2 mm and 5 mm length, respectively (Fig. S2, Table 1). Moreover, PA fragments of both ranges 125–500 μm and 500–1000 μm were not uniform in size, having a mean equivalent spherical diameter (d_{eq}) of 266 ± 29 μm and 836 ± 172 μm, respectively. In contrast, 2 mm and 5 mm PET fibers were more uniform in size with mean equivalent diameters d_{eq} of 192 ± 12 μm and 263 ± 5 μm, respectively.

The settling velocity (W) for each type of MP particle and for sediment particles was calculated following Eq. 3 (see "Additional theory" section in the supplementary material). The settling velocity for sediment particles ranged between $W = 8.5 \times 10^{-7}$ m/s to 0.06 m/s. For the three size ranges selected (fine/medium silts, coarse silts, and fine sands), the mean W was $6.77 \bullet 10^{-5}$ m/s, 0.001 m/s and 0.009 m/s, respectively. For MP, W were 0.0040 ± 0.0008 m/s, 0.0200 ± 0.0010 m/s, 0.0060 ± 0.0006 m/s and 0.0010 ± 0.0002 for PA fragments in the range 125–500 μm, PA fragments in the range 500 μm–1000 μm, 2 mm PET fibers and 5 mm PET fibers, respectively (Fig. S2, Table 1). The Rouse numbers [74] for the three sediment size ranges were calculated following Eq. 8 (see "Additional theory" section in the supplementary material). The mean Rouse number resulted in being equal to 0.10 ± 0.02 (corresponding to the wash/suspended load mode of transport) for the fine/medium silts, 2.07 ± 0.33 (corresponding to the suspended load/bed load mode of transport) for the coarse silts, and 14.36 ± 2.31 (corresponding to the bed load mode of transport) for the fine sands.

3.2. The role of aquatic vegetation in MP retention

The normalized MP concentration (C_{MP}/C_{MP_MAX}, where C_{MP_MAX} was the maximum concentration of MP found near the source) decreased along the flume at a decay rate that depended on both the type of MP and the patch length of the vegetated area (L_P). The normalized concentration of PA fragments in the range 125–500 μm decayed with the progressive distance following an exponential trend in the first platform except for the without-vegetation ($L_p/h_w = 0$) and for the smallest vegetation patch cases considered ($L_p/h_w = 2.5$), where C/C_{MAX} was maximum at 50 cm and 75 cm from the injection point, respectively (Fig. 2). The cases $L_p/h_w = 0$ and $L_p/h_w = 2.5$ presented the smallest decrease in PA fragments along the progressive distance X. An increase in the normalized concentration of PA fragments for all L_P was found inside the lagoon, with the greatest increase being $L_p/h_w = 0$ and $L_p/h_w = 2.5$. In the downstream shallow vegetated area, PA fragments had a very low C/C_{MAX} for all the set-ups considered, with a nearly constant value of 0.1 with the progressive distance. For 2 mm PET fibers, the decay rate exhibited an approximately exponential trend for all L_P and only in the case of full vegetated ($L_p/h_w = 10$) was there a slight relative increase in the C/C_{MAX} found inside the lagoon. In contrast to what was found for PA fragments (125–500 μm), 2 mm PET fibers were nearly the same for all set-ups considered, except for the fully-vegetated case ($L_p/h_w = 10$) where the concentration in the first shallow zone was lower than for the other set-ups (Fig. 2).

C/C_{MAX} for both 500–1000 μm PA fragments and 5 mm PET fibers decreased rapidly with the progressive distance for the two experimental conditions tested ($L_p/h_w = 0$ and $L_p/h_w = 10$), reaching the lagoon in very low concentrations (Fig. S4). In particular, the 500–1000 μm PA fragments exhibited an exponential decay trend reaching low $C/C_{MAX} = 0.004$ at the beginning of the first shallow zone for both $L_p/h_w = 0$ and $L_p/h_w = 10$. Inside the lagoon, and in the second shallow zone, the concentration was very low (≤ 6.86 μl/l in all sediment traps). Five-millimeter PET fibers decayed at a slightly lower rate, reaching $C/C_{MAX} = 0$ at the end of the first shallow zone (section P1D, with $C_{MP} = 0$ μl/l for both set-ups $L_p/h_w = 0$ and $L_p/h_w = 10$) and up to the measuring cross-section P1B (with $C_{MP} = 0.76$ μl/l for $L_p/h_w = 10$). No 5 mm PET fibers were detected beyond these measuring cross-sections.

For small PA fragments in the range 125–500 μm, the characteristic distance along X up to where each type of MP was transported (Δ, see

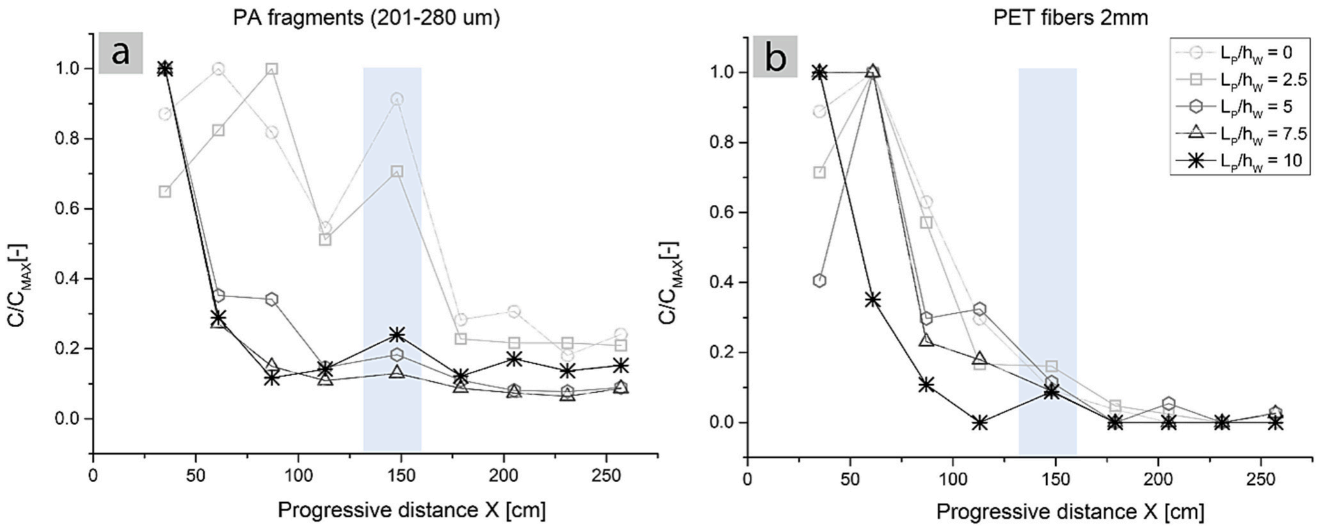

Fig. 2. Normalized MP concentration (C/C_{MAX}) versus the progressive distance X along the main axis of the flume for PA fragments in the range 201–280 μm (a) and 2 mm PET fibers (b) for the different experimental conditions of L_p/h_w tested. The 201–280 μm size range was chosen because it includes the d_{50} of the particle size distribution. The blue area corresponds to the x-position of the lagoon in the flume. (For interpretation of the references to colour in this figure legend, the reader is referred to the web version of this article.)

"Theory section" in the Materials and Methods) decreased as L_P/h_w increased with a sharp decrease of 66 % on average when switching from configurations $L_P/h_w < 2.5$ to $L_P/h_w > 5$ (Fig. 3). For large PA fragments in the 500–1000 μm range, Δ was close to that for 5 mm PET fibers, presenting the lowest values in the lagoon among all the MPs, and remaining approximately constant for both configurations tested ($L_P/h_w = 0$ and $L_P/h_w = 10$, Fig. 3). For 2 mm PET fibers, Δ first increased (with a maximum of $\Delta_{MAX} = 106$ cm for $L_P/h_w = 2.5$) and then decreased up to 72 cm (for $L_P/h_w = 0$). Therefore, only PA fragments sized below 280 μm in the configurations with $L_P/h_w < 2.5$ were able to overcome the lagoon. For all other MP types and L_P, Δ remained below the upstream edge of the lagoon.

3.3. *The role of the lagoon*

The normalized incremental ratio $\frac{(C_i - C_{i-1})/C_{i-1}}{C_{MAX}}$ (where C_i indicates the particle concentration at each measuring section i) was used to compare the evolution of the particle concentration along the progressive distance for the cases with and without lagoon. Positive values of $\frac{(C_i - C_{i-1})/C_{i-1}}{C_{MAX}}$ indicate that the concentration increased with the progressive distance X, whereas negative values indicate a decrease in the concentration with X. For small PA fragments and coarse silt $\frac{(C_i - C_{i-1})/C_{i-1}}{C_{MAX}}$ presented a non-monotonous trend with X, with a high positive value of $\frac{(C_i - C_{i-1})/C_{i-1}}{C_{MAX}}$ at the position of the lagoon (Fig. 4a and b), above $\frac{(C_i - C_{i-1})/C_{i-1}}{C_{MAX}}$ obtained for the case without the lagoon (Fig. 4a and b) for each case, respectively. In contrast, for 2 mm PET fibers, the incremental ratio

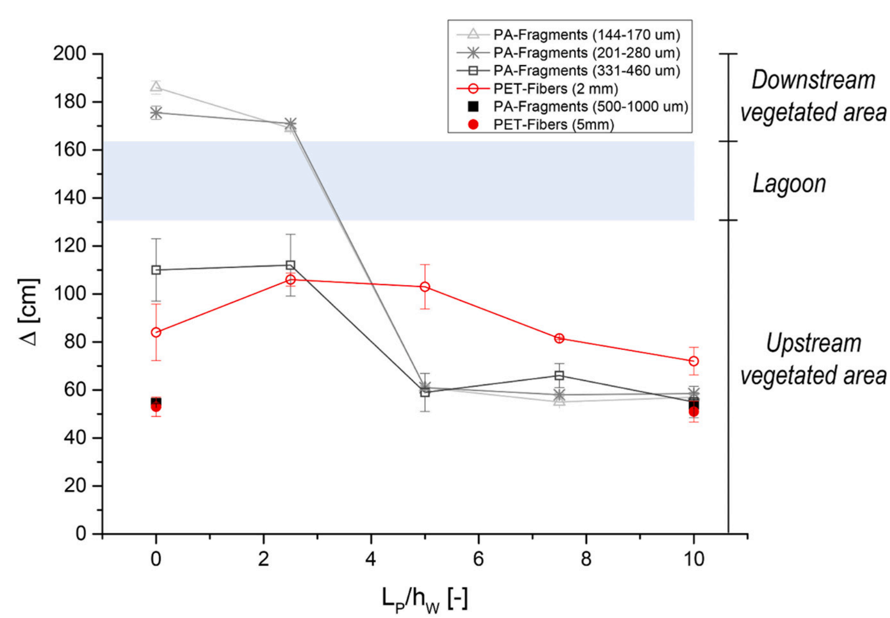

Fig. 3. Horizontal distance Δ (in cm) up to where C/C_{MAX} decreased in a factor e versus the non-dimensional vegetation patch (L_{PATCH}/h_W) for all MP types studied. The blue area represents the positions in x where the lagoon was situated. (For interpretation of the references to colour in this figure legend, the reader is referred to the web version of this article.)

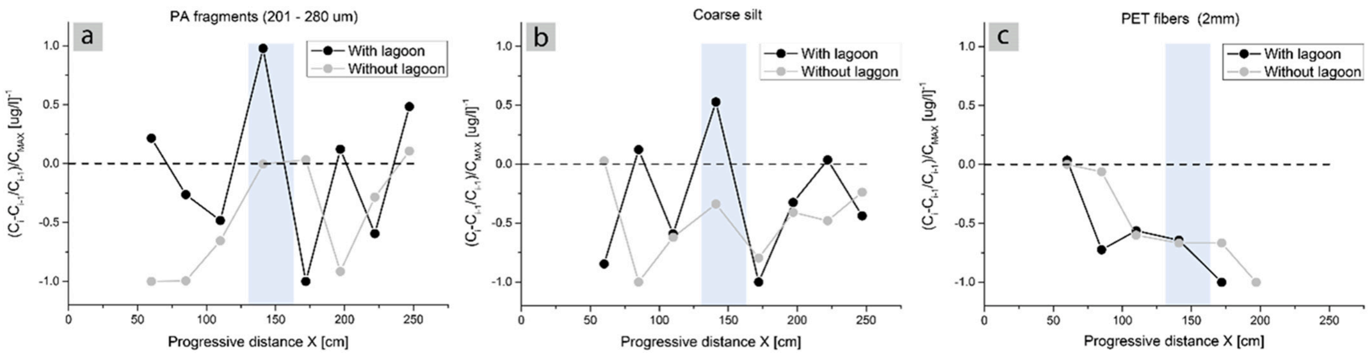

Fig. 4. Normalized incremental ratio $\frac{(C_i - C_{i-1})/C_{i-1}}{C_{MAX}}$ (where C_i indicates the particle concentration at each measuring section i) versus the progressive distance X (in cm) for PA fragments (a), coarse silt (b) and 2 mm PET fibers (c). In each case, experiments with a lagoon have been plotted with those without the lagoon. The blue area represents the positions in x where the lagoon was situated. (For interpretation of the references to colour in this figure legend, the reader is referred to the web version of this article.)

$\frac{(C_i - C_{i-1})/C_{i-1}}{C_{MAX}}$ followed a monotonous decreasing trend with the distance X, with no positive values for either the with-lagoon or without-lagoon cases (Fig. 4c).

Additionally, the normalized MP and suspended sediment (SS) concentrations inside the lagoon (C_L/C_{L_MAX}) depended on both L_P and W of particles (Fig. 5). In general, C_L/C_{L_MAX} decreased as W increased, with different trends with L_P for the different types of particles. Specifically, the maximum concentrations of SS inside the lagoon were found for the fine/medium silts with nearly a constant C_L/C_{L_MAX} for all the configurations considered. An average decrease of 69 % in the C_L/C_{L_MAX} was observed from fine/medium silts (with $W = 6.77 \bullet 10^{-5}$ m/s) to the fine sands (with $W = 0.009$ m/s). PA fragments for the two size ranges 144–170 μm and 201–280 μm had approximately the same C_L/C_{L_MAX} (differing in a 1.5 %). However, C_L/C_{L_MAX} for PA fragments in the 331–460 μm size range decreased by 36 % when compared to the smallest PA fragments. A sharp decrease in C_L/C_{L_MAX} (with an average of 90 %) was observed for the largest PA fragments (in the size range of 500–1000 μm) when compared with the smallest ones. For the largest 5 mm-long PET fibers C_L/C_{L_MAX} was 0, whereas for PET fibers of 2 mm in length C_L/C_{L_MAX} had a mean value of 0.1. For all PA fragments considered, C_L/C_{L_MAX} decreased as L_P increased. For the $L_P/h_W = 0$, C_L/C_{L_MAX} was the highest with $C_L/C_{L\_MAX} \sim 1$, decreasing down to an average of 0.15 among all the size ranges of the PA fragments considered. However, neither fibers of 2 mm nor fibers of 5 mm presented a clear trend with the different vegetation configurations tested. For coarse silts and fine sands, C_L/C_{L_MAX} increased as L_P increased (average increase of 34 % and 122 %, respectively), showing the maximum value for the largest L_P/h_w.

The mean velocity of the plume front (V_{front}) decreased linearly as L_P increased, ranging from 2.48 m/s (for $L_P/h_W = 0$) to 1.66 m/s (for $L_P/h_W = 10$). Following the model proposed in Eq. (2), Δ/L_P decreased with $(W/V_{front}) \bullet CSF$ (Fig. 6b) for all the MP particles and for all the configurations of vegetation surrounding the lagoon considered. Two different regimes can be observed. For $(W/V_{front}) \bullet CSF < 0.05$, Δ/L_P presents a power decrease with $(W/V_{front}) \bullet CSF$. However, for $(W/V_{front}) \bullet CSF > 0.05$ Δ/L_P presents a slower power decrease with $(W/V_{front}) \bullet CSF$

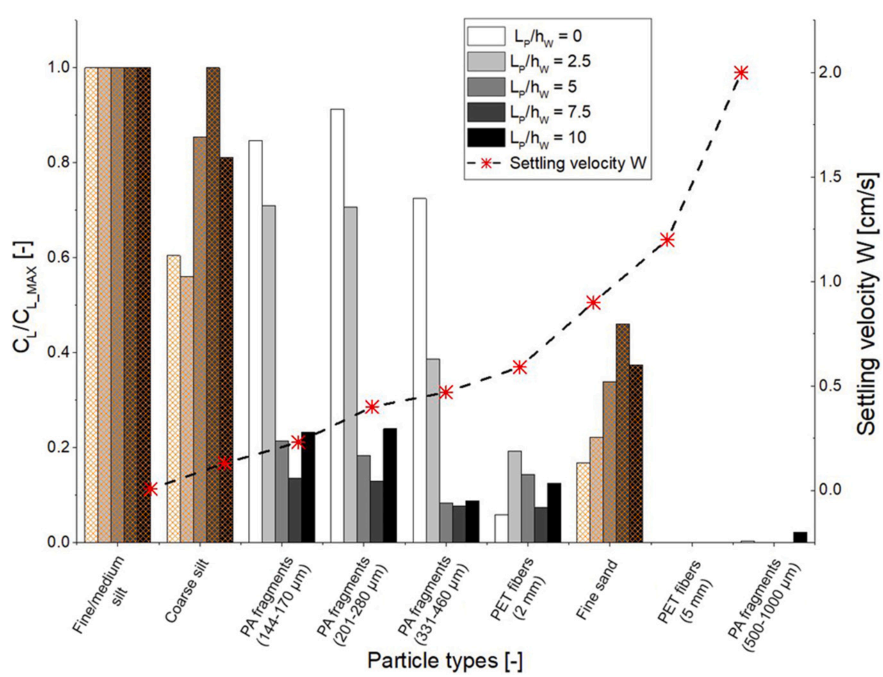

Fig. 5. Normalized concentration (C_L/C_{L_MAX}) of both sediments (orange grid) and MP inside the lagoon for different L_P/h_W values. Red dots represent the calculated settling velocity (W) for each type of particles using the Francalanci et al. [25] formula. The type of particles is ordered from left to right for increasing settling velocities. (For interpretation of the references to colour in this figure legend, the reader is referred to the web version of this article.)

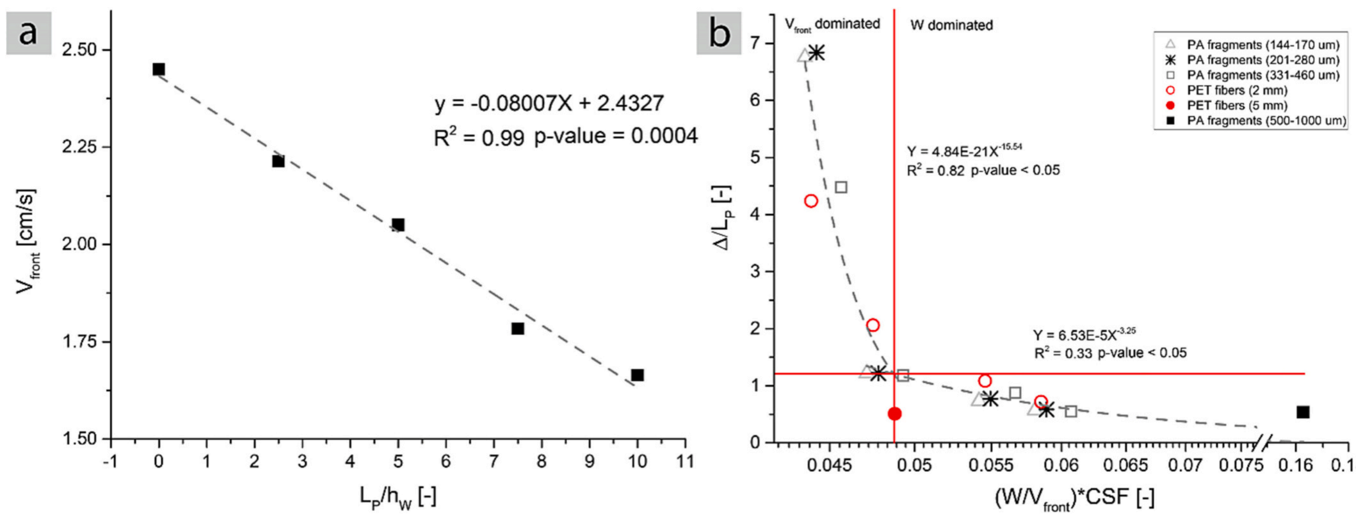

Fig. 6. Relationship between V_{front} (in cm/s) versus the length of the vegetated patch L_P. Relationship between Δ/L_P and $(W/V_{front})\bullet CSF$ for all the experiments carried out. The vertical red line represents the different regimes observed from the data. (For interpretation of the references to colour in this figure legend, the reader is referred to the web version of this article.)

compared to the case $(W/V_{front})\bullet CSF < 0.05$ (Fig. 6b). In addition, for $(W/V_{front})\bullet CSF < 0.05$, MP particles reached the lagoon, meanwhile for $(W/V_{front})\bullet CSF > 0.05$ MPs did not reach the lagoon.

4. Discussion

Natural and constructed wetlands are heterogeneous aquatic systems composed of bare soil areas, vegetated areas, and interspersed deep zones or lagoons, providing complex local hydrodynamics that can be crucial in determining their role in providing ecological services. Emerging contaminants like microplastics are not usually transported alone, instead they are transported along with other particles by river plumes, flooding events, surface run-off, meltwater run-off, glacial drainage, etc. [57]. Besides, they are also vectors for the transport of chemicals associated to the production of plastic materials [58]. In constructed wetlands, wastewater flows with a mixture of sludge and MP particles [59,60]. In the current study, the transport of MP by a particle laden sediment plume was studied. The combination of lagoons interspersed within vegetated areas has been found to retain the migration of MP depending on the characteristics of the MP (shape, size, and density) and the length of the vegetated patches surrounding the lagoon.

4.1. Effect of the vegetation in protecting the lagoon from microplastics

Lagoons retained MP originating from particle laden sediment/MP plumes. However, the presence of vegetation surrounding lagoons provides an additional mechanism in the capacity of retaining MP migration. The presence of the vegetation increased the dispersion of the plume in the lateral direction (compared to the case without plants), therefore increasing the path length of MP and enhancing sedimentation. Lateral dispersion was observed through a reduction in the velocity of the front of the sediment/MP plume as it traveled through the vegetated region. The longer the vegetated patch, the greater the reduction in the velocity of the front. The lateral diffusion of a fluorescent dye in a vegetated area has also been observed in a vegetated model flume where the dispersion increased with the vegetation density [49,61].

4.2. Retention of MP in the lagoon

MP with very high settling velocities (> 1 cm/s, for instance 5 mm PET fibers or PA fragments of sizes over 500 μm), independent of their shape and of the presence of the vegetation, did not reach the lagoon because they settled to the bottom near the injection point. This indicates that MP with high settling velocities will settle close to their sources [21,62]. PA fragments with d < 500 μm had a lower settling velocity compared to large MP and their concentration decreased exponentially along the flume, reaching the lagoon in the cases where the vegetation patch was small ($L_p/h_w < 5$). Therefore, small, vegetated patches were not able to completely retain small PA fragments of d < 500 μm. In addition, the presence of suspended sediments found in the lagoon was also regarded as an additional factor in explaining the retention of slow-settling MP by fast-settling sediment particles through the scavenging mechanism [21]. However, the concentration of PA fragments inside the lagoon decreased as L_P/h_W increased, with a mean reduction rate of 80 % between $L_P/h_W \leq 2.5$ and $L_P/h_W \geq 5$. This implies that vegetated patches play an important role in retaining PA fragments, with an optimal $L_P/h_W = 5$ value beyond which the lagoon could be considered protected from the arrival of PA fragments and all the chemicals that might be bonded to their surface. However, in this study, only a vegetation density was considered for all the experiments performed. The velocity of the front of the plume decreased with the vegetated patch length. Therefore, the presence of vegetation produced an increase in the path length of the plume, as was also described by Nepf et al. [49] for the diffusion of a plume of dye. Furthermore, it should be noted that the type of emergent vegetation used in this work is composed of stems without leaves or emerging roots. The presence of leaves or roots is expected to enhance the capture of MP particles.

The smallest PET fibers (2 mm in length) were mainly retained by the vegetated patch but, unlike the PA fragments, they did not accumulate in the lagoon (only 10 % reached the lagoon). This different behavior can be attributed to the greater settling velocity of PET fibers compared to that of PA fragments. Likewise, vegetated patches increased the lateral dispersion, i.e., increased the path length of migrating particles, retaining PET fibers at the bottom before reaching the lagoon. In the case of $L_P/h_W = 0$, the fact that PET fibers did not accumulate within the lagoon was attributed to the fact that they were more advected due to the high velocities of the front. Likewise, Mancini et al. [21] observed that low distances in certain cases correlated with a high concentration of floating fibers not being able to settle. In their study, this holds when fibers are transported alone, without suspended sediments. In contrast, in the present work, the velocity of the front for the without-plants case transported fibers far from the source, reaching the end of the second platform; probably because there was less dispersion, and the paths of particles were reduced compared to the vegetated cases.

4.3. Implications of the combined effects of vegetation and interspersed lagoons in retaining MP

Floating PET fibers were more likely to be trapped within the vegetated area due to the increase in the path length compared to the without-vegetation case and also because of their high settling velocity. In contrast, small PA fragments (d < 500 μm) did not settle within the shallow vegetated area, but rather accumulated in the lagoon instead as a result of the low flow velocities inside the lagoon. Only in some cases with short vegetation patches ($L_P/h_w < 2.5$) did the smallest PA fragments of d < 280 μm cross over the downstream edge of the lagoon. The presence of the downstream vegetated region after the lagoon produced an additional retention of particles, demonstrating that the combination of deep-water areas interspersed within aquatic vegetation can reduce the percentage of MP migrating from a particle-laden flow. The percentage of MP reduction was calculated as the area below the curve of C/C_{MAX} with the progressive distance X (Table 2). Small PA fragments (d < 500 μm) were reduced by >85 % (88 ± 3 %) at the end of the simulated wetland (lagoon + vegetated areas), and 2 mm PET fibers presented a 99 % (99 ± 1.5 %) reduction. In contrast, without the presence of the lagoon, MP retention was expected to be reduced by 74 ± 6.4 % for small PA fragments and by 93 ± 2.1 % for 2 mm PET fibers. However, for the without-vegetated patches case, PA fragments were reduced by 74 ± 15 % and by 98 ± 1.5 % for 2 mm PET fibers.

Combining the results of all the experimental runs, two different regimes in the transport of MP along the model wetland could be identified: with a threshold between regimes at $(W/V_{front})\bullet CSF = 0.05$. For $(W/V_{front})\bullet CSF < 0.05$, Δ/L_P strongly increased as $(W/V_{front})\bullet CSF$ decreased, indicating that MPs in this regime would be those transported to further distances. This behavior would correspond to MP with low settling velocities compared to the velocity of the front, or likewise to low CSF MP. Low CSF MP corresponds to the case of fibers that, due to their elongated shape, might be oriented with the streamlines of the flow and travel farther. In the current study, however, the fibers used had high settling velocities as so counteracted the effect of CSF. This explains why fibers settled near the source despite having low CSF values. Contrary to this, for $(W/V_{front})\bullet CSF > 0.05$ Δ/L_P decreased with $(W/V_{front})\bullet CSF$, corresponding to those MPs that had been deposited near the source. This would correspond to MPs with high settling velocities compared with the velocity of the front or high CSF.

In summary, vegetated patches are expected to retain particles with high sedimentation rates, whereas lagoons are expected to retain particles with lower sedimentation rates. The combination of vegetated areas and deep-water zones (or lagoons) was found to maximize not only microplastic but also sediment retention. It must be noted that the interaction between sediments and microplastics is crucial in enhancing the flux of MP to the bed [21]. These findings provide information that may help future management strategies for constructed wetlands. In other words, lagoons surrounded by vegetation are potential Nature-Based Solutions (NBS) for reducing MP contamination in streams or rivers. It should be noted that the different mechanisms of particle retention in lagoons compared to vegetated regions produced a differential settling of MP, with different types of MP in each compartment.

4.4. Comparison with other MP retention methodologies

Findings also showed that the MP elimination rates in the combined system tested in this work (88 ± 3 % - 99 ± 1.5 %) are comparable to - if not better than - those of the most common filtration systems used for wastewater treatments (Table 3). For example, membrane bioreactors (MBR) produced MP elimination rates of 82 % for MP particles and MP fibers in the 500–5000 μm size rage [63], while sand filtration methods produce elimination rates in the range of 73.8–99.2 % [64]. MP elimination rates for horizontal subsurface flow treatment systems have been reported to be 88 % [48], supporting the fundamental role vegetation has in increasing MP retention in constructed wetlands [65]. In their work, Cole et al. [66] proposed a NBS based on the use of mussels (*M. galloprovincialis*) to filter polystyrene microbeads which resulted in an elimination rate of about 80 %, nevertheless they found that mussel filtration rates were affected by the age, size, and health of the individuals and by most of the environmental parameters making further improvements to the technique necessary.

MP accumulation in wetlands represents a negative ecological service that should be considered when implementing wastewater treatment plants based on CW. On the other hand, CW can retain MPs and reduce their release into rivers and, consequently, into oceans, which is highly beneficial for these water receptors. However, this also implies that these CW will become highly MP-contaminated areas, storing MP particles coming from both wastewater and stormwater also for a long time [67]. Removal processes of such MPs retained in these shallow engineered water systems could become difficult given that MP degradation and fragmentation break down the particles into smaller and smaller sizes, making them harder to intercept. Moreover, larger MP that is not able to infiltrate deep down into sediment under low water heights [21], might then be resuspended during high flow events. Therefore,

Table 3
Comparison of MP retention percentages for different wastewater treatment systems.

MP type	Kind of removal process	Retained percentage [%]	Reference
PA fragments (125–1000 μm) and PET fibers (2 mm, 5 mm)	CW (deep water zone + vegetation)	88 ± 3–99 ± 1.5	Present study
PET, PS, PE, PP (fragments, fibers, 65.5–500 μm)	Membrane bioreactor (MBR)	95	[63]
PE,PP,PET,PS (particles, fibers, 50–5000 μm)	Sand filtration methods	73.8–99.2	[64]
Fibers, particles, films (40–5600 μm)	Horizontal subsurface flow treatment systems	88	[48]
PP,PET,PS,PES,PA,PE, POM (fragments, fibers, granules, 0.03–5 mm)	Rural domestic wastewater treatment facilities (RC-WWTFs)	42–84	[65]
PS and PE-S spheres, PA-S and PA-L fibers, PE-L and PP granules (10–100 μm)	*M. galloprovincialis*	80	[66]

Table 2
Percentage of MP retained in the system combining the effects of the lagoon and vegetation by varying L_P/h_W. Percentages were calculated as the area below the curve C/C_{MAX} with the progressive distance X. * In this case particles remained floating along the flume (see the discussion section for more details).

Mean MP percentage retained [%] in the model wetland										
	PA Fragments (125–500 μm)					*PET fibers (2 mm)*				
L_P/h_W	*0*	*2.5*	*5*	*7.5*	*10*	*0*	*2.5*	*5*	*7.5*	*10*
Shallow vegetated zone	64.9	69.0	79.3	80.7	68.6	95.6	91.3	91.2	95.4	94.3
shallow zone + lagoon	87.9	87.9	90.8	90.7	84.3	100*	99.1	96.3	99	100

future ad-hoc management procedures should be designed, investigated and applied to maintain the good ecological status of CWs and their efficiency.

In addition, as natural wetlands have been proven to trap MP from the sea into inland areas or from the rivers to the sea, they are expected to be plastic pollution hot spots. Considering that they are valuable areas in terms of biodiversity, this might represent a threat to all the organisms living in these areas.

5. Conclusion

In this study, a simulated lagoon interspersed between two vegetated shallow water areas was found to accumulate MP fragments, with relatively low sedimentation rates, from a particle-laden sediment plume. This work has proved that when a lagoon is surrounded by emergent aquatic vegetation (here *Juncus maritimus*), the concentration of MP fragments in the lagoon decreased as the length of the vegetated area increased. The concentration of MP fragments presented a mean reduction rate of 80 % between $L_P/h_W \leq 2.5$ and $L_P/h_W \geq 5$. Moreover, vegetated patches were also able to trap MP fibers and this increased as the patch length increased indicating that in natural wetlands, aquatic vegetation plays a fundamental role in protecting lagoons from MP pollution.

Additionally, findings from this study reveal that wetlands with interspersed lagoons sheltered by vegetation are suitable to be used as nature-based solutions for treating contaminated water with MP released from punctual sources, and that only a combination of deep-water areas and aquatic vegetation is required to maximize the retention rates of different MP types. The percentages are comparable to those of the most common filtration systems.

The outcomes highlight the significance of the present work in developing more efficient strategies for maintaining and preserving natural wetlands from plastic pollution, and in providing guidance to optimize nature-based solution systems encompassing constructed wetlands.

Declaration of competing interest

The authors declare that they have no known competing financial interests or personal relationships that could have appeared to influence the work reported in this paper.

Data availability

Data will be made available on request.

Acknowledgments

This work was supported by the Ministerio de Economía y Competitividad of the Spanish Government through Grant PID2021-123860OB-I00. We are grateful to the University of Girona Research Technical Services and the Grup de Recerca en Materials i Termodinàmica of the University of Girona for all the technical assistance provided to develop this project. We would also like to thank Pere Bellvehí for the technical help provided, and Joan Bassachs for providing PA MP.

Appendix A. Supplementary data

Supplementary data to this article can be found online at https://doi.org/10.1016/j.jwpe.2023.104559.

References

[1] C. Wang, J. Zhao, B. Xing, Environmental Source, Fate, and Toxicity of Microplastics, in: Journal of Hazardous Materials, 407, Elsevier B.V., 2021, https://doi.org/10.1016/j.jhazmat.2020.124357.
[2] A. Isobe, S. Iwasaki, The fate of missing ocean plastics: are they just a marine environmental problem? Sci. Total Environ. 825 (2022) https://doi.org/10.1016/j.scitotenv.2022.153935.
[3] L.C.M. Lebreton, J. Van Der Zwet, J.W. Damsteeg, B. Slat, A. Andrady, J. Reisser, River plastic emissions to the world's oceans, Nat. Commun. 8 (2017), https://doi.org/10.1038/ncomms15611.
[4] C. Schmidt, T. Krauth, S. Wagner, Export of plastic debris by Rivers into the sea, Environ. Sci. Technol. 51 (21) (2017) 12246–12253, https://doi.org/10.1021/acs.est.7b02368.
[5] E. Hengstmann, E. Weil, P.C. Wallbott, M. Tamminga, E.K. Fischer, Microplastics in lakeshore and lakebed sediments – external influences and temporal and spatial variabilities of concentrations, Environ. Res. 197 (February) (2021), 111141, https://doi.org/10.1016/j.envres.2021.111141.
[6] Y. Zhang, K. Wang, W. Chen, Y. Ba, K. Khan, W. Chen, C. Tu, C. Chen, L. Xu, Effects of land use and landscape on the occurrence and distribution of microplastics in soil, China, Sci. Total Environ. 847 (2022), https://doi.org/10.1016/j.scitotenv.2022.157598.
[7] J. Gasperi, R. Dris, T. Bonin, V. Rocher, B. Tassin, Assessment of floating plastic debris in surface water along the Seine River, Environ Pollut. 195 (2014) 163–166, https://doi.org/10.1016/j.envpol.2014.09.001.
[8] L.J.J. Meijer, T. Van Emmerik, R. Van Der Ent, C. Schmidt, L. Lebreton, More than 1000 rivers account for 80% of global riverine plastic emissions into the ocean, Sci. Adv. 7 (2021). https://www.science.org.
[9] D. Morritt, P.V. Stefanoudis, D. Pearce, O.A. Crimmen, P.F. Clark, Plastic in the Thames: a river runs through it, Mar. Pollut. Bull. 78 (1–2) (2014) 196–200, https://doi.org/10.1016/j.marpolbul.2013.10.035.
[10] T. van Emmerik, Y. Mellink, R. Hauk, K. Waldschläger, L. Schreyers, Rivers as plastic reservoirs, Front. Water 3 (2022), https://doi.org/10.3389/frwa.2021.786936.
[11] L. Gallitelli, G. Di Lollo, C. Adduce, M.R. Maggi, B. Trombetta, M. Scalici, Aquatic plants entrap different size of plastics in indoor flume experiments, Sci. Total Environ. 863 (2023), https://doi.org/10.1016/j.scitotenv.2022.161051.
[12] D.K.A. Barnes, F. Galgani, R.C. Thompson, M. Barlaz, Accumulation and fragmentation of plastic debris in global environments, Philos. Trans. R. Soc. B 364 (1526) (2009) 1985–1998, https://doi.org/10.1098/rstb.2008.0205.
[13] A. Mateos-Cárdenas, J. O'Halloran, F.N.A.M. van Pelt, M.A.K. Jansen, Rapid fragmentation of microplastics by the freshwater amphipod Gammarus duebeni (Lillj.), Sci. Rep. 10 (1) (2020), https://doi.org/10.1038/s41598-020-69635-2.
[14] Y.K. Song, S.H. Hong, M. Jang, G.M. Han, S.W. Jung, W.J. Shim, Combined effects of UV exposure duration and mechanical abrasion on microplastic fragmentation by polymer type, Environ. Sci. Technol. 51 (8) (2017) 4368–4376, https://doi.org/10.1021/acs.est.6b06155.
[15] M. Bergmann, L. Gutow, M. Klages, Marine anthropogenic litter, Mar. Anthrop. Litter 1–447 (2015), https://doi.org/10.1007/978-3-319-16510-3.
[16] J. Sun, H. Zheng, H. Xiang, J. Fan, H. Jiang, The surface degradation and release of microplastics from plastic films studied by UV radiation and mechanical abrasion, Sci. Total Environ. 838 (2022), https://doi.org/10.1016/j.scitotenv.2022.156369.
[17] K. Waldschläger, M. Born, W. Cowger, A. Gray, H. Schüttrumpf, Settling and rising velocities of environmentally weathered micro- and macroplastic particles, Environ. Res. 191 (2020), https://doi.org/10.1016/j.envres.2020.110192.
[18] Y. Yan, F. Zhu, C. Zhu, Z. Chen, S. Liu, C. Wang, C. Gu, Dibutyl phthalate release from polyvinyl chloride microplastics: influence of plastic properties and environmental factors, Water Res. 204 (2021), https://doi.org/10.1016/j.watres.2021.117597.
[19] J. Glüge, N.M. Ashta, D. Herzke, L. Lebreton, M. Scheringer, Correspondence regarding the Perspective "Addressing the importance of microplastic particles as vectors for long-range transport of chemical contaminants: perspective in relation to prioritizing research and regulatory actions.", Microplast. Nanoplast. 2 (1) (2022) 1–19, https://doi.org/10.1186/s43591-021-00021-z.
[20] T. Serra, J. Colomer, Scavenging of polystyrene microplastics by sediment particles in both turbulent and calm aquatic environments, Sci. Total Environ. 884 (2023), https://doi.org/10.1016/j.scitotenv.2023.163720.
[21] M. Mancini, T. Serra, J. Colomer, L. Solari, Suspended sediments mediate microplastic sedimentation in unidirectional flows, Sci. Total Environ. 890 (2023), https://doi.org/10.1016/j.scitotenv.2023.164363.
[22] R. Kumar, P. Sharma, A. Verma, P.K. Jha, P. Singh, P.K. Gupta, R. Chandra, P. V. Vara Prasad, Effect of Physical Characteristics and Hydrodynamic Conditions on Transport and Deposition of Microplastics in Riverine Ecosystem, in: Water (Switzerland), Vol. 13, Issue 19, MDPI, 2021, https://doi.org/10.3390/w13192710.
[23] A. Ballent, S. Pando, A. Purser, M.F. Juliano, L. Thomsen, Modelled transport of benthic marine microplastic pollution in the Nazaré Canyon, Biogeosciences 10 (12) (2013) 7957–7970, https://doi.org/10.5194/bg-10-7957-2013.
[24] K. Critchell, J. Lambrechts, Modelling accumulation of marine plastics in the coastal zone; what are the dominant physical processes? Estuar. Coast. Shelf Sci. 171 (2016) 111–122, https://doi.org/10.1016/j.ecss.2016.01.036.
[25] S. Francalanci, E. Paris, L. Solari, On the prediction of settling velocity for plastic particles of different shapes, Environ. Pollut. 290 (2021), https://doi.org/10.1016/j.envpol.2021.118068.
[26] De Wit, R. (n.d.). 2 Biodiversity of Coastal Lagoon Ecosystems and Their Vulnerability to Global Change. www.intechopen.com.
[27] A. Pérez-Ruzafa, I.M. Pérez-Ruzafa, A. Newton, C. Marcos, Coastal lagoons: environmental variability, ecosystem complexity, and goods and services uniformity, in: Coasts and Estuaries: The Future, Elsevier, 2019, pp. 253–276, https://doi.org/10.1016/B978-0-12-814003-1.00015-0.

[28] O. Garcés-Ordóñez, J.F. Saldarriaga-Vélez, L.F. Espinosa-Díaz, M. Canals, A. Sánchez-Vidal, M. Thiel, A systematic review on microplastic pollution in water, sediments, and organisms from 50 coastal lagoons across the globe, in: Environmental Pollution vol. 315, Elsevier Ltd., 2022, https://doi.org/10.1016/j.envpol.2022.120366.
[29] L. Simon-Sánchez, M. Grelaud, J. Garcia-Orellana, P. Ziveri, River deltas as hotspots of microplastic accumulation: the case study of the Ebro River (NW Mediterranean), Sci. Total Environ. 687 (2019) 1186–1196, https://doi.org/10.1016/j.scitotenv.2019.06.168.
[30] A.L.G. Camargo, P. Girard, C. Sanz-Lazaro, A.C.M. Silva, É. de Faria, B.R. S. Figueiredo, D.S. Caixeta, M.C.M. Blettler, Microplastics in sediments of the Pantanal Wetlands, Brazil, Front. Environ. Sci. 10 (2022), https://doi.org/10.3389/fenvs.2022.1017480.
[31] J. Kee, H. Wong, K. Kin, K. Ho, D. Tang, P. Yap, Microplastics in the freshwater and terrestrial environments: prevalence, fates, impacts and sustainable solutions, Sci. Total Environ. 719 (2020), 137512, https://doi.org/10.1016/j.scitotenv.2020.137512.
[32] H.C. Lu, S. Ziajahromi, P.A. Neale, F.D.L. Leusch, A systematic review of freshwater microplastics in water and sediments: recommendations for harmonisation to enhance future study comparisons, Sci. Total Environ. 781 (2021), 146693, https://doi.org/10.1016/j.scitotenv.2021.146693.
[33] R. Mao, Y. Hu, S. Zhang, R. Wu, X. Guo, Microplastics in the surface water of Wuliangsuhai Lake, northern China, Sci. Total Environ. 723 (2020), https://doi.org/10.1016/j.scitotenv.2020.137820.
[34] F. Gbogbo, J.B. Takyi, M.K. Billah, J. Ewool, Analysis of microplastics in wetland samples from coastal Ghana using the Rose Bengal stain, Environ. Monit. Assess. 192 (4) (2020), https://doi.org/10.1007/s10661-020-8175-8.
[35] M. Mistri, M. Scoponi, A.A. Sfriso, C. Munari, M. Curiotto, A. Sfriso, M. Orlando-Bonaca, L. Lipej, Microplastic contamination in protected areas of the Gulf of Venice, Water Air Soil Pollut. 232 (9) (2021), https://doi.org/10.1007/s11270-021-05323-9.
[36] L. Cozzolino, K.R. Nicastro, G.I. Zardi, C.B. de los Santos, Species-specific plastic accumulation in the sediment and canopy of coastal vegetated habitats, Sci. Total Environ. 723 (2020), https://doi.org/10.1016/j.scitotenv.2020.138018.
[37] A.A. Sfriso, Y. Tomio, A.S. Juhmani, A. Sfriso, C. Munari, M. Mistri, Macrophytes: a temporary sink for microplastics in transitional water systems, Water (Switzerland) 13 (21) (2021), https://doi.org/10.3390/w13213032.
[38] R. Md Amin, E.S. Sohaimi, S.T. Anuar, Z. Bachok, Microplastic ingestion by zooplankton in Terengganu coastal waters, southern South China Sea, Mar. Pollut. Bull. 150 (2020), https://doi.org/10.1016/j.marpolbul.2019.110616.
[39] J. Bayo, D. Rojo, P. Martínez-Baños, J. López-Castellanos, S. Olmos, Commercial gilthead seabream (Sparus aurata L.) from the Mar Menor coastal lagoon as hotspots of microplastic accumulation in the digestive system, Int. J. Environ. Res. Public Health 18 (13) (2021), https://doi.org/10.3390/ijerph18136844.
[40] S. Pradit, P. Noppradit, P. Jitkaew, K. Sengloyluan, M. Yucharoen, P. Suwanno, V. Tanrattanakul, K. Sornplang, T. Nitiratsuwan, Microplastic accumulation in catfish and its effects on fish eggs from Songkhla lagoon, Thailand, J. Mar. Sci. Eng. 11 (4) (2023), https://doi.org/10.3390/jmse11040723.
[41] S. Abidli, M. Pinheiro, Y. Lahbib, T. Neuparth, M.M. Santos, N. Trigui, E. Menif, Effects of Environmentally Relevant Levels of Polyethylene Microplastic on *Mytilus galloprovincialis* (Mollusca: Bivalvia): Filtration Rate and Oxidative Stress, 2021, https://doi.org/10.1007/s11356-021-12506-8/Published.
[42] J. Ding, C. Sun, J. Li, H. Shi, X. Xu, P. Ju, F. Jiang, F. Li, Microplastics in Global Bivalve Mollusks: A Call for Protocol Standardization, in: Journal of Hazardous Materials, vol. 438, Elsevier B.V., 2022, https://doi.org/10.1016/j.jhazmat.2022.129490.
[43] L. Zhong, T. Wu, H.J. Sun, J. Ding, J.W. Pang, L. Zhang, N.Q. Ren, S.S. Yang, Recent Advances Towards Micro(nano)plastics Research in Wetland Ecosystems: A Systematic Review on Sources, Removal, and Ecological Impacts, in: Journal of Hazardous Materials, 452, Elsevier B.V., 2023, https://doi.org/10.1016/j.jhazmat.2023.131341.
[44] R. Helcoski, L.T. Yonkos, A. Sanchez, A.H. Baldwin, Wetland soil microplastics are negatively related to vegetation cover and stem density, Environ. Pollut. 256 (2020), https://doi.org/10.1016/j.envpol.2019.113391.
[45] T. Serra, E. Font, M. Soler, A. Barcelona, J. Colomer, Mean residence time of lagoons in shallow vegetated floodplains, Hydrol. Process. 35 (2) (2021), https://doi.org/10.1002/hyp.14065.
[46] D.J. Sarkar, S. Das Sarkar, B.K. Das, B.K. Sahoo, A. Das, S.K. Nag, R.K. Manna, B. K. Behera, S. Samanta, Occurrence, fate and removal of microplastics as heavy metal vector in natural wastewater treatment wetland system, Water Res. 192 (2021), https://doi.org/10.1016/j.watres.2021.116853.
[47] Y. Chen, T. Li, H. Hu, H. Ao, X. Xiong, H. Shi, C. Wu, Transport and fate of microplastics in constructed wetlands: a microcosm study, J. Hazard. Mater. 415 (2021), https://doi.org/10.1016/j.jhazmat.2021.125615.
[48] Q. Wang, C. Hernández-Crespo, M. Santoni, S. Van Hulle, D.P.L. Rousseau, Horizontal subsurface flow constructed wetlands as tertiary treatment: can they be an efficient barrier for microplastics pollution? Sci. Total Environ. 721 (2020) https://doi.org/10.1016/j.scitotenv.2020.137785.
[49] H.M. Nepf, J.A. Sullivan, R.A. Zavistoski, A model for diffusion within emergent vegetation, Lirwrol. ocetrrro~r 42 (8) (1997).
[50] A. Barcelona, T. Serra, J. Colomer, Fragmented canopies control the regimes of gravity current development, J. Geophys. Res. Oceans 123 (3) (2018) 1631–1646, https://doi.org/10.1002/2017JC013145.
[51] L.A. Leonard, M.E. Luther, Flow hydrodynamics in tidal marsh canopies, Limnol. Oceanogr. 40 (8) (1995) 1474–1484, https://doi.org/10.4319/lo.1995.40.8.1474.
[52] D. Pujol, J. Colomer, T. Serra, X. Casamitjana, Effect of submerged aquatic vegetation on turbulence induced by an oscillating grid, Cont. Shelf Res. 30 (9) (2010) 1019–1029, https://doi.org/10.1016/j.csr.2010.02.014.
[53] D. Pujol, T. Serra, J. Colomer, X. Casamitjana, Flow structure in canopy models dominated by progressive waves, J. Hydrol. 486 (2013) 281–292, https://doi.org/10.1016/j.jhydrol.2013.01.024.
[54] X. Casamitjana, D. Pujol, J. Colomer, T. Serra, Application of a k-ε formulation to model the effect of submerged aquatic vegetation on turbulence induced by an oscillating grid, Cont. Shelf Res. 34 (2012) 1–6, https://doi.org/10.1016/j.csr.2011.11.003.
[55] À. Ros, J. Colomer, T. Serra, D. Pujol, M. Soler, X. Casamitjana, Experimental observations on sediment resuspension within submerged model canopies under oscillatory flow, Cont. Shelf Res. 91 (2014) 220–231, https://doi.org/10.1016/j.csr.2014.10.004.
[56] C.K. Wentworth, A Scale of Grade and Class Terms for Clastic Sediments, 1922.
[57] B. He, M. Smith, P. Egodawatta, G.A. Ayoko, L. Rintoul, A. Goonetilleke, Dispersal and transport of microplastics in river sediments, Environ. Pollut. 279 (2021), https://doi.org/10.1016/j.envpol.2021.116884.
[58] T. Gouin, Addressing the importance of microplastic particles as vectors for long-range transport of chemical contaminants: perspective in relation to prioritizing research and regulatory actions, Micropl. & Nanopl. 1 (2021) 14, https://doi.org/10.1186/s43591-021-00016-w.
[59] F. Bydalek, D. Ifayemi, L. Reynolds, R. Barden, B. Kasprzyk-Hordern, J. Wenk, Microplastic dynamics in a free water surface constructed wetland, Sci. Total Environ. 858 (2023), https://doi.org/10.1016/j.scitotenv.2022.160113.
[60] C. Nie, J. Yang, C. Sang, Y. Xia, K. Huang, Reduction performance of microplastics and their behavior in a vermi-wetland during the recycling of excess sludge: a quantitative assessment for fluorescent polymethyl methacrylate, Sci. Total Environ. 832 (2022), https://doi.org/10.1016/j.scitotenv.2022.155005.
[61] T. Serra, H.J.S. Fernando, R.V. Rodríguez, Effects of emergent vegetation on lateral diffusion in wetlands, Water Res. 38 (1) (2004) 139–147, https://doi.org/10.1016/j.watres.2003.09.009.
[62] M. Pinheiro, I. Martins, J. Raimundo, M. Caetano, T. Neuparth, M.M. Santos, Stressors of emerging concern in deep-sea environments: microplastics, pharmaceuticals, personal care products and deep-sea mining, Sci. Total Environ. 876 (2023), 162557, https://doi.org/10.1016/j.scitotenv.2023.162557.
[63] X. Lv, Q. Dong, Z. Zuo, Y. Liu, X. Huang, W.M. Wu, Microplastics in a municipal wastewater treatment plant: fate, dynamic distribution, removal efficiencies, and control strategies, J. Clean. Prod. 225 (2019) 579–586, https://doi.org/10.1016/j.jclepro.2019.03.321.
[64] S. Wolff, F. Weber, J. Kerpen, M. Winklhofer, M. Engelhart, L. Barkmann, Elimination of microplastics by downstream sand filters in wastewater treatment, Water (Switzerland) 13 (1) (2021), https://doi.org/10.3390/w13010033.
[65] S. Wei, H. Luo, J. Zou, J. Chen, X. Pan, D.P.L. Rousseau, J. Li, Characteristics and removal of microplastics in rural domestic wastewater treatment facilities of China, Sci. Total Environ. 739 (2020), https://doi.org/10.1016/j.scitotenv.2020.139935.
[66] M. Cole, Y. Artioli, R. Coppock, G. Galli, R. Saad, R. Torres, T. Vance, A. Yunnie, P. K. Lindeque, Mussel power: scoping a nature-based solution to microplastic debris, J. Hazard. Mater. 453 (2023), https://doi.org/10.1016/j.jhazmat.2023.131392.
[67] H.C. Lu, S. Ziajahromi, A. Locke, P.A. Neale, F.D.L. Leusch, Microplastics profile in constructed wetlands: distribution, retention and implications, Environ. Pollut. 313 (September) (2022), 120079, https://doi.org/10.1016/j.envpol.2022.120079.
[74] H. Rouse, Modern conceptions of mechanics of fluid turbulence, ASCE 102 (1937) 463–505.